БЪЛГАРКА АКАДМИЯ НА НАУКИТ BULGARIAN ACADEMY OF S NCS
ТЕОРЕТИЧНА И ПРИЛОЖНА МЕХАНИКА THEORETICAL AND APPLIED MHANICSC
София, 1989, год. XX, № 2 Sofia, 1989, Year XX, No 2

Numerical Study of Steady Flow past Two Equal Cylinders at Moderate Reynolds Numbers

Tz. Kotzev, Z. Zapryanov, E. Toshev

1. Introduction

One of the most deeply studied problems in viscous hydrodynamics deals with the steady-state flow past a circular cylinder in an otherwise uniform stream. Despite the apparent simplicity of the geometry of this problem, a closed form exact solution appears to be permanently out of reach. However, there exist some approximate solutions for the steady flow past a cylinder.

In many practical cases the flow field is affected not only by the cylinder but also by the presence of rigid walls or free surfaces. In some cases the situation is such that two-cylinder hydrodynamic interactions have to be considered.

In 1955 Takaisi [1] studied on the basis of Oseen's equations of motion the steady slow motion of a circular cylinder in a viscous liquid bounded by two parallel plane walls when the cylinder is moving midway between the bounding walls. It was shown that at sufficiently small Reynolds numbers the drag on the cylinder is independent of the Reynolds number, i. e., it is of the so-called Stokes type, as was shown by White experiments [2] on wires falling in viscous liquids between two vertical plates. The forces acting on two circular cylinders of arbitrary radii placed in tandem orientation in a uniform stream at low Reynolds numbers were calculated by Fujikawa [3].

The same author has also calculated the forces acting on two equal circular cylinders placed side by side in an uniform stream at low Reynolds number. It was found that the individual cylinder experiences a smaller drag when the two cylinders are in tandem orientation than when they are placed side by side. In 1954 Imai [4] proposed a new analytical method for solving the Oseen's equations. On the basis of this method he investigated the uniform flow past an elliptic cylinder at an arbitrary angle of incidence and obtained the expressions for the velocity distribution near the elliptic cylinder as well as for the drag and lift up to a second approximation. Using Imai's general method of solving two-dimensional Oseen's equations Kuwabara calculated the forces experienced by two circular [5] and two elliptic [6] cylinders placed in a uniform flow at small values of Reynolds numbers.

In 1979 Dorrepaal and O'Neill [7] studied the Stokes flow past two equal circular cylinders in contact and not in contact where the direction of flow is perpendicular to the line joining the centres. They found Moffat [8] vortices in bipolar coordinates when the cylinders are in contact. The steady two-dimensional Stokes flow past two circular cylinders of equal radii, when the direction of the flow is parallel to the line joining the centers, was considered by Miyazaki and Hasimoto [9]. They have

calculated the separation of the creeping flow and found confined eddies near the boundary of a wall or body.

Since some properties of the viscous fluid flow past an obstacle cannot be fully explained by an analysis based on the Stokes or Oseen approximation, one must take into account the nonlinear terms in the Navier-Stokes equations. Recent years have witnessed a renaissance of numerical methods which is linked with the tremendous advance in highspeed computers. The obtained numerical solutions are based on finite-difference representations of the equations governing the fluid motion. The degree of approximation in such kinds of representations depends on a large number of factors including the basic differentiating method, mesh sizing, boundary conditions, and stability and convergence criteria used to obtain the solution.

Few areas in fluid mechanics have received more attention than that of flow past a circular cylinder. Numerical solutions for steady flow of viscous incompressible fluid past a circular cilinder were reported by Tom [10] for Reynolds numbers up to 20, Kawaguti [11] for Re=40 and Allen and Southwell [12] for Re=1—100. More recently, Fornberg [13] has obtained numerical solutions for steady, viscous flow past a circular cylinder at Reynolds number up to 300. He proposed a new technique for the boundary condition at large distances and an iteration scheme based on Newton's method which circumvents the numerical difficulties previously encountered around and beyond a Reynolds number of 100. Numerical solution of the problem of steady flow around an elliptic cylinder for Re=40 has been obtained by Dennis and Chang [14].

In spite of many numerical methods and calculations, the Reynolds number Re=100 (based on the cylinder diameter) appears to be the upper limit for which complete, steady flow fields have been reliably determined because steady solutions for the circular cylinder become experimentally unstable around Re=40. The unsteady flow around an elliptic cylinder at various angles of attack was investigated by Patel [15].

In 1973 Bearman and Wadcock [16] described an experimental investigation of the flow about a pair of circular cylinders separated in a plane normal to the free stream. They studied the way in which the flows past the cylinders changed, as their separation is reduced from that past two independent cylinders to that past a single body. The bipolar coordinate solution of the two-dimensional Stokes equations was applied by Wakiya [17] to flows around the circular cylinders. Solutions were presented in three cases for a cylinder revolving eccentrically in a cylindrical frame, a cylinder in the neighbourhood of a plane wall and two cylinders in rotary motion as a pair. In 1982 Umemura [18] reported matched-asymptotic analysis of low-Reynolds-number flow past two equal circular cylinders. He overcame the difficulties of this problem by considering the flow field far from the cylinders and then modifying the solution near the cylinders so that it becomes the inner expansion for an application of the method of matched asymptotic expansions. A numerical implementation of the method of matched asymptotic expansions was proposed by Lee and Leal [19] to analyze two-dimensional uniform streaming flow at low Reynolds numbers past a straight cylinder (or two cylinders) of arbitrary cross-sectional shape.

A numerical solution of the problem of cross flow past two circular cylinders in line at moderate Reynolds numbers has been carried out by Belov and Kudryavtzev [20]. With this investigation they formed an idea of the mechanism and the pattern of the flow between and around two circular cylinders, and explained the mutual influence of the cylinders on the characteristic changes of the drag. Using the same method Md. S. Alam et al. [21] solved in the same 1981 the following problems: a) flow past two square cylinders; b) flow past two circular cylinders. In the same paper they also solved the axisymmetric problem of flow past spheres under periodic boundary conditions.

In the present paper the method of numerical matching is developed for solving the problem of viscous, incompressible flow past two equal elliptic cylinders in tandem

arrangement at moderate Reynolds numbers. The main attention is focused in the calculation of the hydrodynamic interaction between two cylinders for different values of the Reynolds number and axis ratio $k=b/a$. Two cases are considered in particular:

(i) The uniform flow and the cylinder major axes are parallel;

(ii) The uniform flow and the cylinder major axes are perpendicular.

2. Formulation of the problem

Let us consider an uniform stream with velocity U_0 at infinity which impinges on two equal elliptic cylinders of major and minor axes a, b respectively and with parallel axes separated by a distance d (Fig. 1).

In terms of the usuat Cartesian coordinates (x', y'), the equations relating the pressure p and the velocity components (v_x', v_y') for two-dimensional incompessible flow are:

$$v_x' \frac{\partial V_x'}{\partial x'} + v_y' \frac{\partial v_x'}{\partial y'} = -\frac{1}{\rho}\frac{\partial p'}{\partial x'} + \nu\left(\frac{\partial^2 v_x'}{\partial x'^2} + \frac{\partial^2 v_x'}{\partial y'^2}\right)$$

$$v_x' \frac{\partial v_y'}{\partial x'} + v_y' \frac{\partial v_y'}{\partial y'} = -\frac{1}{\rho}\frac{\partial p'}{\partial y'} + \nu\left(\frac{\partial^2 v_y'}{\partial x'^2} + \frac{\partial^2 v_y'}{\partial y'^2}\right)$$

$$\frac{\partial v_x'}{\partial x'} + \frac{\partial v_y'}{\partial y'} = 0,$$

where ρ is density and ν kinematic viscosity.

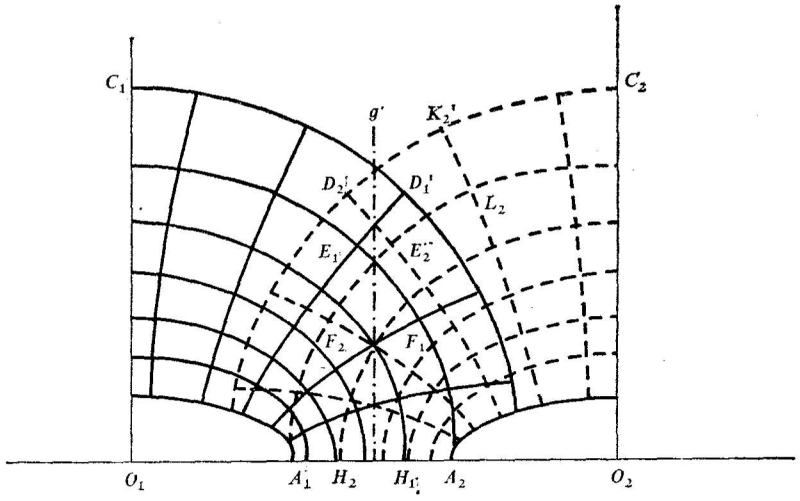

Fig. 1

It is well known that one can obtain a solution of these equations for fhe flow past two bodies when there exists such a coordinate system in which the two body surfaces are coordinate surfaces. The chief advantage of such coordinate system is that one can satisfy the boundary conditions in an easy manner. Due to the lack of suitable coordinate system, the flow past two elliptic cylinders at moderate Reynolds

numbers remains unsettled until now. In this study we shall solve this problem by extending the new method of numerical matching [20, 21] utilizing two elliptic coordinate systems suitable for each single cylinder. We suppose that each of the two elliptic coordinate systems (ξ, η) is fixed with one of the cylinders and is defined by the transformation:

$$x'+iy'=C\cosh(\xi+i\eta),$$

where C is a positive constant and $0\leq\xi<\infty$, $0\leq\eta<2\pi$. So, the two considered equal elliptic cylinders are defined by $\xi=\xi_0$. With U_0 as a typical velocity and a as a typical geometrical length we can introduce the non-dimensional variables according to the scheme:

$$x=\frac{x'}{a},\quad y=\frac{y'}{a},\quad \psi=\frac{\psi'}{aU_0},\quad Re=\frac{2aU_0}{\nu}, \tag{1}$$

where ψ is non-dimensional Stokes'stream function and Re — Reynolds number.

The equation of continuity in an elliptic coordinate system has the form

$$\frac{\partial}{\partial\xi}(hv_\xi)+\frac{\partial}{\partial\eta}(hv_\eta)=0, \tag{2}$$

where $h=\operatorname{sech}\xi_0(\cosh^2\xi-\cos^2\eta)^{\frac{1}{2}}$. Then the velocity components v_ξ and v_η are expressed in terms of the stream function ψ as follows:

$$v_\xi=+\frac{1}{h}\frac{\partial\psi}{\partial\eta},\quad v_\eta=+\frac{1}{h}\frac{\partial\psi}{\partial\xi}. \tag{3}$$

In order to find the numerical solution of governing equations to the plane flow past two elliptic cylinders we shall use stream-function-vorticity formulation of the problem:

$$\frac{1}{h^2}\left(\frac{\partial\psi}{\partial\xi}\frac{\partial\zeta}{\partial\eta}-\frac{\partial\psi}{\partial\eta}\frac{\partial\zeta}{\partial\xi}\right)=\frac{2}{Re}\nabla^2\zeta, \tag{4}$$

$$\nabla^2\psi=\zeta, \tag{5}$$

where ζ is the vorticity and $\nabla^2\equiv\frac{1}{h^2}\left(\frac{\partial^2}{\partial\xi^2}+\frac{\partial^2}{\partial\eta^2}\right)$. Although the flow is considered to be in an infinite medium, it is not possible to perform the numerical analysis in an infinite domain. The field of computation is therefore restricted by an external elliptic envelope which, like the elliptic curve, coincides with the elliptic coordinate grid lines. It is convenient to seek instead of the stream function ψ a new unknown function $\tilde{\psi}$, which is related to ψ as

$$\psi=\tilde{\psi}+\operatorname{sec}h\,\xi_0\,\sinh\xi\sin\eta. \tag{6}$$

Here the second term of the right hand side is due to the uniform flow and $\tilde{\psi}$ is the deviation of the actual flow from the former. Then the velocity equation (5) becomes

$$\nabla^2\tilde{\psi}=\zeta. \tag{7}$$

The boundary conditions are:

$$\tilde{\psi}=-\operatorname{sec}h\,\xi_0\sinh\xi\sin\eta \quad \text{at } \xi=\xi_0 \tag{8}$$

$$\tilde{\psi}=\zeta=0 \quad \text{at } \xi=\xi_\infty,\ \eta=0,\ \pi. \tag{9}$$

The drag on a body is expressed in terms of a dimensionless drag coefficient $C_D = \frac{\text{drag}}{\frac{1}{2}\rho U_0^2 a}$. The total drag coefficient is composed of two parts: the pressure drag coefficient and the skin drag coefficient, i. e.: $C_D = C_{DP} + C_{DF}$,

where

$$C_{DF} = -\frac{4}{Re}\int_0^{\pi} \zeta_0 \sin\eta d\eta$$

$$C_{DP} = \frac{4}{Re}\,\tanh \xi_0 \int_0^{\pi} \left(\frac{\partial\zeta}{\partial\xi}\right)_{\xi=\xi_0} \sin\eta\, d\eta.$$

We shall note that for the case when the uniform flow and the cylinder axes are perpendicular the governing equations could be obtained from those when the uniform flow and the cylinder axes are parallel by replacing each $\cosh\xi$ by $i\sinh\xi$ and each $\sinh\xi$ by $i\cosh\xi$.

3. Finite difference approximation and computational procedure

The rapid changes of the stream function and the vorticity in the vicinity of leading and trailing edges of the cylinders require small mesh size while in the regions far from the bodies rather large mesh size may be used. This graduation of mesh size is conveniently achieved by transforming the physical plane into the elliptic coordinates (ξ, η). In the numerical procedure the infinite domain of integration past each cylinder is replaced by a finite network of points determined by $\{\xi_i = \xi_0 + i\Delta\xi, \eta_j = j\Delta\eta\}$, where $\Delta\xi$ and $\Delta\eta$ are increments in ξ and η lines respectively and $i = 0, 1, 2, \ldots, M$, $j = 0, 1, 2, \ldots, N$.

The main difficulties associated with the solution of the Navier-Stokes equations in stream-function vorticity formulation of the above problem are the following:

(a) There is a lack of boundary condition for the vorticity over the cylinders.
(b) The pressure is not directly obtained and additional calculations are required for its determination.

The solution of the steady equations (4) and (5) is obtained for large values of the fictitious times t_1 and t_2 in the equations:

$$\frac{\partial\xi}{\partial t_1} + \frac{1}{h_2}\left(\frac{\partial\psi}{\partial\xi}\frac{\partial\zeta}{\partial\eta} - \frac{\partial\psi}{\partial\eta}\frac{\partial\zeta}{\partial\xi}\right) = \frac{2}{Re}\nabla^2\zeta \tag{10}$$

and the equation

$$\frac{\partial\tilde{\psi}}{\partial t_2} = \nabla^2\tilde{\psi} - \zeta. \tag{11}$$

The system of equations of evolution is solved by the method of fractional steps. It is evident that the equation (11) has no physical meaning before the steady state is reached.

The advantage of such formulation is that we have two parabolic equations and a step-by-step economical scheme can be used in contrast to formulation (4), (5) where the elliptic equations have to be solved.

For the first half-time step in the (i, j) mesh node one has

$$\frac{\zeta_{i,j}^{n+\frac{1}{2}}-\zeta_{i,j}^{n}}{0.5\Delta t_1}=\Lambda_\xi\zeta_{i,j}^{n+\frac{1}{2}}-\Lambda_\eta\zeta_{i,j}^{n} \tag{12}$$

and for the second half-time step

$$\frac{\zeta_{i,j}^{n+1}-\zeta^{n+\frac{1}{2}}}{0.5\Delta t_1}=\Lambda_\xi\zeta_{i,j}^{n+\frac{1}{2}}-\Lambda_\eta\zeta_{i,j}^{n+1}, \tag{13}$$

where Δt_1 is time step and

$$\Lambda_\xi\zeta_{i,j}=\frac{1}{8\Delta\xi\Delta\eta}\{\zeta_{i+1,j}(\psi_{i+1,j+1}+\psi_{i,j+1}-\psi_{i+1,j-1}-\psi_{i,j-1})+\zeta_{i,j}(\psi_{i+1,j+1}+\psi_{i-1,j-1}$$
$$-\psi_{i+1,j-1}-\psi_{i-1,j+1})-\zeta_{i-1,j}(\psi_{i,j+1}+\psi_{i-1,j+1}-\psi_{i,j-1}-\psi_{i-1,j-1})\}+$$
$$+\frac{2}{Re(\Delta\xi)^2}(\zeta_{i+1,j}-2\zeta_{i,j}+\zeta_{i-1,j})$$

$$\Lambda_\eta\zeta_{i,j}=\frac{1}{8\Delta\xi\Delta\eta}\{\zeta_{i,j+1}(\psi_{i+1,j+1}+\psi_{i+1,j}-\psi_{i-1,j+1}-\psi_{i+1,j})+\zeta_{i,j}(\psi_{i+1,j+1}+\psi_{i-1,j-1}$$
$$-\psi_{i-1,j+1}-\psi_{i+1,j-1})-\zeta_{i,j-1}(\psi_{i+1,j-1}+\psi_{i+1,j}-\psi_{i-1,j}-\psi_{i-1,j-1})\}$$
$$+\frac{2}{Re(\Delta\eta)^2}(\zeta_{i,j+1}-2\zeta_{i,j}+\zeta_{i,j-1}).$$

The equation (10) can be approximated with the usual five-point scheme as follows

$$\frac{\tilde{\psi}_{i,j}^{n+\frac{1}{2}}-\tilde{\psi}_{i,j}^{n}}{0.5\Delta t_2}=\frac{\delta_\xi^2\tilde{\psi}_{i,j}^{n+\frac{1}{2}}}{(\Delta\xi)^2}+\frac{\delta_\lambda^2\tilde{\psi}_{i,j}^{n}}{(\Delta\eta)^2}-\zeta_{i,j}h_{i,j}^2 \tag{14}$$

$$\frac{\tilde{\psi}_{i,j}^{n+1}-\tilde{\psi}_{i,j}^{n+\frac{1}{2}}}{0.5\Delta t^2}=\frac{\delta_\xi^2\tilde{\psi}_{i,j}^{n+\frac{1}{2}}}{(\Delta\xi)^2}+\frac{\delta_\eta^2\tilde{\psi}_{i,j}^{n+1}}{(\Delta\eta)^2}-\zeta_{i,j}h_{i,j}^2, \tag{15}$$

where Δt_2 is time step and

$$\delta_\xi^2\tilde{\psi}_{i,j}=\tilde{\psi}_{i+1,j}-2\tilde{\psi}_{i,j}+\tilde{\psi}_{i-1,j},\quad \delta_\eta^2\tilde{\psi}_{i,j}=\tilde{\psi}_{i,j+1}-2\tilde{\psi}_{i,j}+\tilde{\psi}_{i,j-1}.$$

We shall note again that the approximated fictitious derivative in time has no physical meaning and serves to the chosen numerical method.

After approximating the boundary conditions (8), (9), we get

$$\tilde{\psi}_{0,j}=-\sec h\,\xi_0\sin h\,\xi_0\sin,\eta_j,\quad \xi=\xi_0$$
$$\tilde{\psi}_{M,j}=0,\qquad \xi=\xi_\infty$$
$$\tilde{\psi}_{i,0}=\tilde{\psi}_{i,N}=\zeta_{i,0}=\zeta_{i,N}=0,\qquad \eta=0,\ \pi$$

$i=0, 1, 2, \ldots, M$; $j=0, 1, 2, \ldots, N$.

Following the first-order Thom's formula [10], one can construct boundary condition for vorticity ζ as follows:

$$\zeta_{0,j}^{n+1}=\frac{2\psi_{1,j}^{n+1}}{h_{0,j}^2(\Delta\xi)^2}\omega+(1-\omega)\zeta_{0,j}^{n}, \tag{16}$$

where ω is the relaxation parameter and indices "0" and "n" denote the cylinder surface and time step respectively. The optimum value of the parameter ω is found to be of the order min $(\Delta\xi, \Delta\eta)$. In the present paper $\omega=0.05$. Since the flow at infinity $(\xi=\xi_\infty)$ is undisturbed we suppose that

$$\zeta_{M,j}=0 \quad \text{for } J=0,\ 1,\ 2,\ \ldots,\ N.$$

In this way one obtains a linear system of algebraic equations with a three-diagonal matrix which can be solved using the Gaussian elimination.

A great number of details must be taken into account concerning the interaction between two bodies which is connected with the application of the method of numerical matching. In order to apply this method we divide the area around two elliptic cylinders into two subdomains using the straight line g which is perpendicular to the line $O_1O_2=0$ and intersects it at the middle of the distance between two cylinders.

The essence of the method of numerical matching is that the equations of motion are solved separately for each cylinder in such a way that the obtained solutions overlap in a previously chosen zone between the bodies. It consists of difference grid points which are chosen in the following way. For example, in the first subregion, for each coordinate line $\eta=\text{const}$ which intersects the straight line g there exists a grid point D_1, placed at the right side of the line g. Let D_1 is located among four grid points K_2, L_2, E_2, and D_2 of the second mesh. Then in order to give an account of the influence of the second cylinder on the first one, for the parameter f of the flow ($f\equiv\tilde{\psi}$, $f\equiv\zeta$) one can calculate f_{D_1} by the equation

$$f_{D_1}=l_{K_2}f_{K_2}+l_{L_2}f_{L_2}+l_{E_2}f_{E_2}+l_{D_2}f_{D_2}, \tag{17}$$

where l_{K_2}, l_{L_2}, l_{E_2}, l_{D_2} are interpolation coefficients and f_{K_2}, f_{L_2}, f_{E_2}, f_{D_2} are the values of parameter f in the nodes of the second mesh. In such a way we obtain the domain $D_1E_1F_1H_1H_2F_2E_2D_2$, in which the solutions around the two bodies are matched.

The computational procedure is realized by the following algorithm:

1) $\tilde{\psi}=0$ and $\zeta=0$ are adopted as a first approximation of the solutions around the bodies.

2) Calculate from (17) the additional boundary conditions of $\tilde{\psi}$ and ζ in the additional boundary grids for the first subdomain of the flow.

3) Solve the equation (5) in the first subdomain with respect to $\tilde{\psi}$.

4) Calculate from (17) the boundary conditions for $\tilde{\psi}$ and ζ for the second subdomain using the values found for $\tilde{\psi}$.

5) Solve the equation (5) in the second subdomain.

The steps from 2) to 5) are repeated m times until error criterion $\max|\tilde{\psi}^{m+1}_{i,j}-\tilde{\psi}^{m}_{i,j}|\leq 10^{-5}$ is reached.

6) Calculate from (16) the vorticity ζ on the surface of the first cylinder.

7) Solve the equation (4) in order to find ζ in the first subdomain.

8) Calculate from (16) the vorticity ζ on the surface of the second cylinder.

9) Solve the equation (4) in order to find in the second subdomain.

10) For the next step go back to 2).

The main iterative procedure is terminated when the following criterion is satisfied:

$$\max_{i,j}|\zeta^{n+1}_{i,j}-\zeta^{n}_{i,j}|\leq 10^{-4},$$

where $i=0,\ 1,\ 2,\ \ldots,\ M$, $j=0,\ 1,2,\ \ldots N-1$.

The number of the iterations which are necessary to get steady solution depends on the Reynolds number, the separation distance between the cylinders, the width of the overlap domain, etc.

4. Numerical results

The method described above has been applied to study numerically the hydrodynamic interaction between two equal elliptic cylinders in tandem arrangement for different values of the axis ratio, the Reynolds number and the distances between the cylinders.

For all cases in this study we chose $M=N=41$ and the axis ratio is 0.4 and 0.2. The outer boundary is about 50 major axes far from the centres and the steps along ξ and η are respectively $\Delta\xi=0.125$, $\Delta\eta=\pi/40$.

4.1. The hydrodynamic interaction between two equal elliptic cylinders when the uniform flow and the cylinder major axes are parallel [case (*i*)].

The numerical solution of the problem (4)—(9) was obtained for $Re=1$, 5, 40, 60, 80, 212, $k=0.2$, 0.33, 0.4 and the distance between two cylinders $d=0$, 0.25, 0.5, 1, 1.5, 4, 10.

Fig. 2 (*a*, *b*) shows the curves of constant stream function for $k=0.4$ and $Re=80$ when the separation distance d is equal to 1 and 1.5 respectively.

One can see that two shear layers separated by an upstream cylinder attach onto a downstream cylinder and there is an intensive second recirculation zone behind the

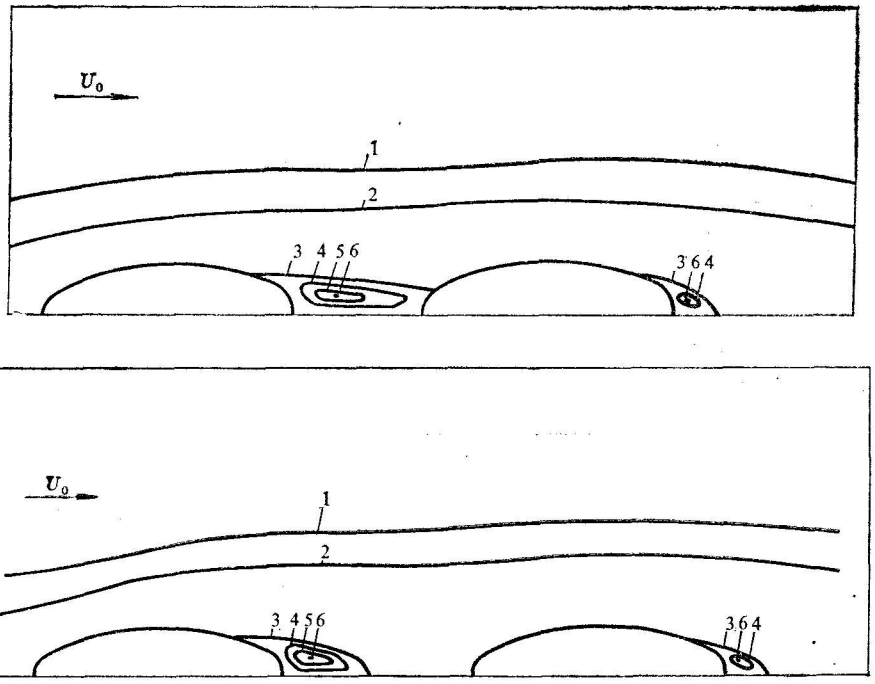

Fig. 2 $Re=80$, $k=0.4$
(*a*) $d=1$
1. −0.5; 2. −0.25, 3. 0; 4. 0.0007, 5. 0.0014; 6. 0.0021
(*b*) $d=1.5$
1. −0.5; 2. −0.25; 3. 0; 4. 0.0005; 5. 0.0009; 6. 0.002

downstream cylinder. When the distance d between the cylinders is not small, the recirculating zone of the upstream cylinder does not contact the downstream one and the flow pattern resembles the flow past a single cylinder. Fig. 3 shows the dependence of the total drag coefficient on the separation distance d between two equal

elliptic cylinders with axis ratios 0.4 and 0.2 for $Re=80$. The numerical results obtained show that the drag force acting on each of the elliptic cylinder is smaller than the drag force experience on a single cylinder and the drag on the upstream one is greater than that on the downstream one. When the separation distance d increases

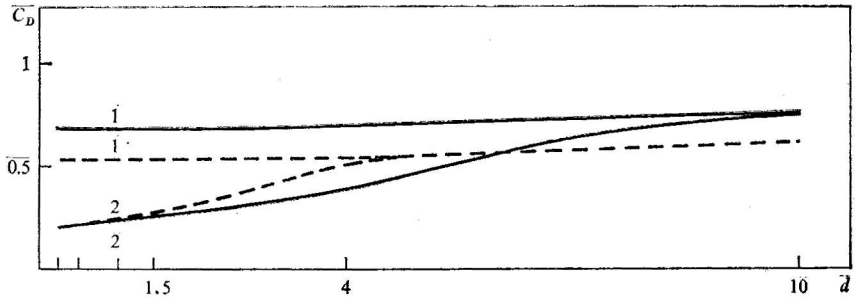

Fig. 3. $Re=80$, —— $k=0,4$, ····· $k=0.2$

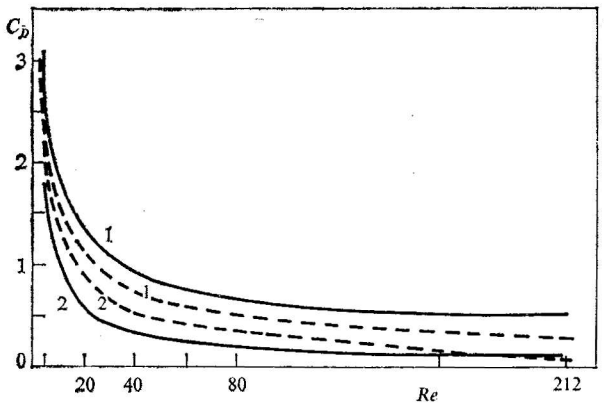

Fig. 4. $d=1$, —— $k=0.4$, ····· $k=0.2$

the drag forces of the two bodies are drawn closer together and when d is about 10 or larger they are practically equal.

It is interesting to note the following experiment: we investigated the stationary flow past two touching elliptic cylinders with a ratio of the semi-axes $k=0.33$ at Reynolds number 212. The sum of drag coefficients of the two bodies differs in the second place after the decimal point from the drag coefficient of an impulsively-starting elliptic cylinder of the same dimensions for great times when the stationary regime of flow is achieved [15]. Consequently, at this Reynolds number the configuration of two touching elliptic cylinders is almost as stream-lined as an elliptic cylinder.

At $Re=40$ and $k=0.4$ the above stated things are not confirmed. Then the sum $C_{D_1}+C_{D_2}$ is greater than the drag coefficient of one elliptic cylinder. The reason is the considerable contribution of friction drag to the total drag whereas for great Reynolds numbers the drag due to the fluid's pressure is prevailing.

In Fig. 4 the drag coefficient of the two equal elliptic cylinders are plotted against Reynolds number for $d=1$. When the Reynolds number increases, the drag coefficients of the two cylinders decrease and the difference between these two coefficients increases with increasing the axis ratio.

It was established by the numerical experiments made that for a distance between the elliptic cylinders $d=1$ and a ratio of semi-axes $k=0.4$ a domain of reverse flow appears behind the first one for $Re=35$. The second body is strongly influenced by the delay of the flow caused by the presence of the other cylinder because a recirculating zone behind it is beginning to be observed as far as $Re=55$.

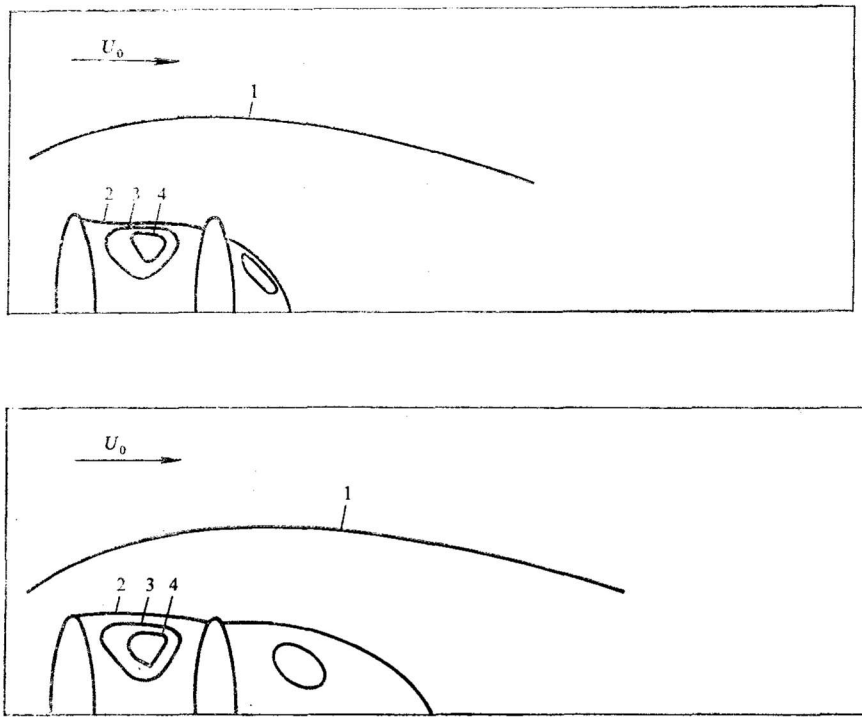

Fig. 5. $d=1$, $k=0.2$
(*a*) $Re=5$
1. −0.5; 2.0; 3. 0.0045; 4. 0.091
(*b*) $Re=20$
1−0.25; 2.0; 3. 0.0064; 4. 0.013

The length of recirculating zone behind the downstream cylinder increases with increasing the separation distance d and tends to the recirculating zone length of a single cylinder at the same flow conditions. The vorticity distribution at the two elliptic cylinder surfaces for $Re=80$, $k=0.4$ and $d=1$ is given in Fig. 8. The maximum absolute value of the vorticity over the two cylinder surfaces is reached at about 156° for the first body and 105° for the second one measured from the rear stagnation point.

4.2. The hydrodynamic interaction between two equal elliptic cylinders when the uniform flow and the cylinder major axes are perpendicular [case (*ii*)].

Fig. 5 (*a, b*) shows the streamline pattern at Reynolds numbers $Re=5$ and 20 for a distance between the cylinders $d=1$ and axes ratio $k=0.4$. The recirculating zone of the upstream cylinder contacts the downstream cylinder and the flow above this zone is forced to move along the surface against an unfavourable pressure gradient. It results in a downstream recirculating zone behind the second cylinder. It is formed for $Re\approx4$ while for $Re=5$ it is in the form shown in Fig. 5a. For elliptic cylinders with a ratio of semi-axes 0.2 the second recirculating zone is formed for $Re\approx2$. The increase of the distance between the elliptic cylinders causes a decrease of the length of the

second recirculating zone. This tendence continues for values of d at which the zone of reverse flow between the bodies separates from the surface of the second one. Then the length of the second recirculating zone increases and equals with that behind the first cylinder.

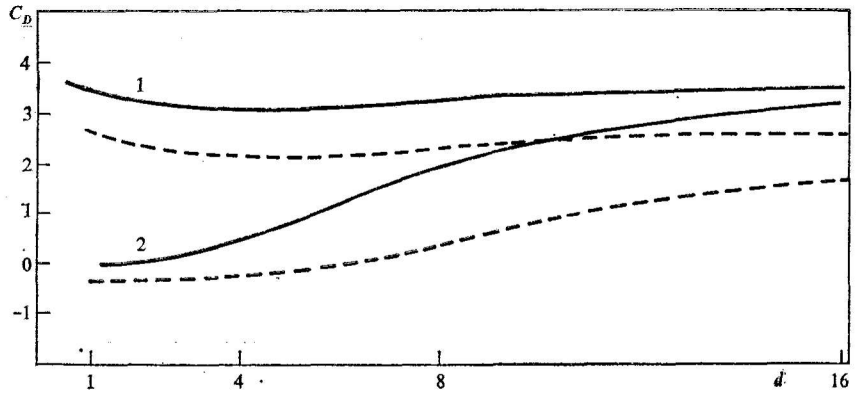

Fig. 6. $k=0.4$, —— $Re=20$, – – – – $Re=40$

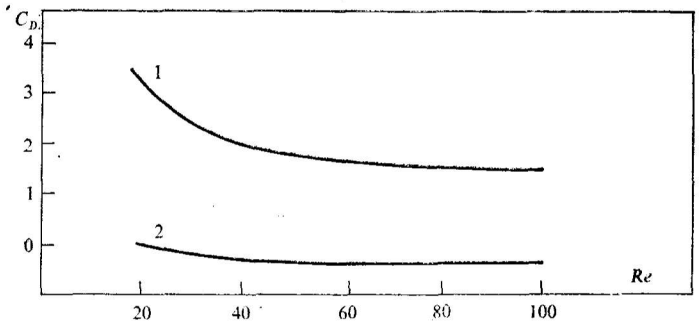

Fig. 7. $d=1$, $k=0.4$

The variation of the drag coefficients of the two elliptic cylinders with a separation distance d for $Re=20$ and 40 can be seen in Fig. 6. When the distance d increases, the drag coefficients for upstream cylinder changes slowly while the drag coefficient of the downstream cylinder varies rapidly due to the interaction between the bodies. A negative value for the drag coefficient of the downstream cylinder appears for small separation distances. It means that when two cylinders are to move freely, the rear one moves towards the upstream cylinder against the direction of the flow.

When the separation distance increases, the drag coefficient of the downstream cylinder increases also and tends to the value of the drag coefficient of an isolated elliptic cylinder.

In Fig. 7 the drag coefficient C_D is plotted against Reynolds number at $d=1$ for a separation distance $d=1$ and axis ratio $k=0.4$. In contrast to the case when the uniform flow and the major axes are parallel, in the case when they are perpendicular, the drag coefficient of the downstream cylinder is negative for Reynolds numbers greater than 25.

The vorticity distribution over the two elliptic cylinder surfaces for $Re=80$, $k=0.4$ and $d=1$ is shown in Fig. 8. One can see a large gradient of the vorticity about the separation point due to the curvature of the body.

To ensure as far as it is possible that the observed features of the flow fields are real and not peculiar to the discrete approximation, we checked the independence

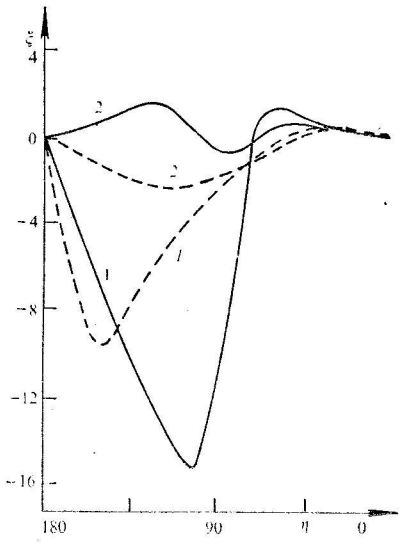

Fig. 8. $Re=80$, $d=1$, $k=0.4$, – – – – case (i), —— case (ii)

of these solutions to changes in the grid sizes. Having the densities of both upstream and downstream grids from 41×41 to 21×21, we offered sufficient resolution power up to a Reynolds number of 212. The discrepancies for the total drag coefficient obtained for these two grids are about 6% both for the upstream cylinder and the downstream one.

In order to check the accuracy of the proposed scheme, we also compared our results with the results of the other authors considering the case of the flow past an elliptic cylinder. When the axis ratio is equal to 0.5, $Re=1$ and the separation distance d is large ($d=16$), our results for the drag coefficient of the upstream and downstream cylinders are 10.22 and 9.03 respectively, while according to I m a i's result [4] for an isolated elliptic cylinder it is 10.21 at first approximation and 9.91 at second approximation. Our results are in excellent agreement with the numerical solution given in [14] for the steady flow past an elliptic cylinder for $Re=40$. Good agreements are also obtained with results in [15]. When $k=1$, we had chances to compare our results with the results given in [20] and [21] and to establish a good agreement.

5. Conclusions

The method of numerical matching has been extended to solve the problem of hydrodynamic interaction between two equal elliptic cylinders in tandem arrangement at moderate Reynolds numbers. The main attention is focused on the study of the hydrodynamic interaction between two equal elliptic cylinders in tandem arrangement for different values of the axis ratio, Reynolds number and the distances between two cylinders. Two cases are considered:

(i) The uniform flow and the elliptic cylinder major axes are parallel;
(ii) The uniform flow and the elliptic cylinder major axes are perpendicular.

It has been found that when the Reynolds number is small, the interactions between the cylinders fade away rapidly when they are placed at large distances. If the Reynolds number is moderate, the interactions are large even when the cylinders are not placed at small distances. For moderate Reynolds numbers and not so large separation distance two shear layers separated from the upstream cylinder attach onto the downstream one and there is an intensive second recirculation zone behind the downstream cylinder. When the distance between the cylinders is not small, the recirculating zone of the upstream cylinder does not contact the downstream one and the flow pattern resembles the flow past an isolated elliptic cylinder.

The numerical results obtained show that the drag coefficient of each of the considered elliptic cylinders is smaller than the drag coefficient of a single elliptic cylinder in the same flow conditions. The drag coefficient of the upstream cylinder is greater than the drag coefficient of the downstream one. In contrast to the case when the uniform flow and the major axes are parallel, in the case when they are perpendicular, a negative value of the drag coefficient of the downstream cylinder appears in some cases. It means that when two cylinders are to move freely, the downstream one moves to the upstream cylinder against the direction of the flow.

In conclusion, it can be said that the proposed scheme of the method of numerical matching appears to be a capable tool for solving the problems of viscous flow past two bodies.

References

1. Takaisi, Y. — J. Phys. Soc., Japan, 1955, 10, 685.
2. White, C. M. — Proc. Roy. Soc., A 186, 1946, 472.
3. Fujikawa, H. — J. Phys. Soc., Japan, 1956, 11, 690.
4. Imai, I. — Proc. Roy. Soc., 1954, A 224, 141.
5. Kuwabara, S. — J. Phys. Soc., Japan, 1957, 12, 291.
6. Kuwabara, S. — J. Phys. Soc., Japan, 1958, 5, 506.
7. Dorrepaal, J. M., M. E. O'Neill. — Q. J. Mech. Appl. Math., 1979, XXXII, 95.
8. Moffat, H. K. — J. Fluid Mech., 1964, 18, 1.
9. Miyazaki, T., H. Hasimoto. — J. Phys. Soc., Japan, 1980, 49, 1611.
10. Thom, A. — Proc. Roy. Soc., London, 1933, A 141, 651.
11. Kawaguti, M. — J. Phys. Soc., Japan, 1953, 8, 747.
12. Allen, D. N., R. V. Southwell. — Q. J. Mech. and Appl. Math., 1955, 8, 129.
13. Fornberg, B. A. — J. Fluid Mech., 1980, 98, 819.
14. Dennis, S. C. R., G. Z. Chang. — Phys. Fluids Suppl., 1969, 12, 88.
15. Patel, V. A. — Comp. Fluids., 1981, 9, 435.
16. Bearman, P. W., A. J. Wadcock. — J. Fluid Mech., 1973, 61, 499.
17. Wakiya, S. — J. Phys. Soc., Japan, 1975, 39, 603.
18. Umemura, A. — J. Fluid Mech. — 1982, 121, 345.
19. Lee, S. H., L. G. Leal. — J. Fluid Mech., 1986, 164, 401.
20. Belov, I. A., N. A. Kudryavtzev. — Eng. Phys. J. — 1981, 2, 310.
21. Alam, Md. S., T. Kawamura, K. Kuwahara, H. Takami. Preprints of JSME Meeting., 1981, Tokyo.

Received 7 December 1988